Optimization of Laser Ablation Parameters for Lumbar Discectomy

Robert Delgado, Mohamed Hassan, Shaumik Ashraf, William Chan

Keywords: Laser discectomy, herniated disc, lumbar pain, intervertebral disc, ablation

In partial fulfillment of the requirements for BEE 4530
Computer Aided Engineering: Applications to Biological Systems

Department of Biological and Environmental Engineering
Cornell University

Table of Contents

1. Executive Summary

Lower back pain, or lumbar pain, is a potentially debilitating chronic condition that will affect an estimated 80% of individuals in their lifetime. Lumbar pain can be caused by herniated lumbar discs, which is a painful ailment that occurs when the nucleolus pulposus or annulus fibrosus of an intervertebral lumbar disc is displaced beyond the intervertebral space and pinches the spinal nerve. The resulting nervous stimulation produces tremendous localized pain in the lower back and, in some cases, referred pain in the legs or arms.

Current methods that can treat herniated discs include physical therapy, epidural steroid injections, and surgical removal. The former two solutions only treat mild cases of lumbar disc herniation, and the latter solution has a long recovery time with postoperative complications. The application of laser discectomy to the treatment of lumbar pain associated with herniated discs is not novel; lasers have been used as a minimally-invasive treatment of moderately severe cases of herniated discs since the late 20^{th} century.

This study aims to analyze and improve minimally invasive laser ablation to remove lumbar disc tissue that has been displaced from its proper position. Concentrating an infrared laser beam on the herniated part of the intervertebral disc causes vaporization of the tissue with unparalleled precision. This results in relieved pressure on the spinal nerve and alleviation of pain. Two parameters in laser surgery are power density and separation between pulses, which must be manipulated to minimize surgery time and reduce collateral thermal affliction.

Using COMSOL Multiphysics® a herniated intervertebral disc and adjacent vertebrae was designed for laser ablation and transient heating analysis. A 3-dimensional Cartesian geometry was adopted and modeled with conductive heat transfer coupled with volumetric laser-heat generation determined by optical diffusion. The laser ablation physics was modeled by implementing a velocity at nodes that have reached the ablation temperature.

The method of evaluating the effectiveness of the simulation is through determination of the mass loss via ablation due to the total energy transferred. This would ensure safe ablation of tissue during a laser discectomy surgery and lower the risk of protein denaturation, excessive water loss (reducing intervertebral disc shock absorption), and irreversible changes to tissue functionality as a result of changes in material properties. As a result, post-operative complications can be evaded and overall treatment of lumbar disc herniation (LDH) will become more efficient. Furthermore, this computational modeling approach was chosen in order to study the effect and impact of parameter variation on the laser ablation procedure, and to computationally optimize the length of the procedure to allow for mass loss with minimal thermal damage to healthy tissue.

Results of this study indicate that mass loss begins at approximately 6.2 seconds, after the temperature of the tissue has been raised to the ablation temperature. Sensitivity analysis of the model revealed that the mass loss is most dependent on the density of the intervertebral tissue and the power of the laser applied. Optimization of the laser ablation surgery occurs at 10.9 seconds, when the difference between the amount of herniated intervertebral damaged and the

amount of healthy intervertebral disc and vertebral bone tissue damaged is maximized. More anatomically accurate computational models can be generated by using meshes of CT scans of the intervertebral disc, manually building various types of hernias and then running the same analysis of finding optimal laser parameters. Non-negligible vapor flow resulting from laser ablation can also be incorporated into future models.

Keywords: Laser discectomy, herniated disc, lumbar pain, intervertebral disc, ablation

2. Introduction

Lower back pain, or lumbar pain, is an often debilitating injury characterized by pronounced nervous system stimulation. Such pain can be triggered by degeneration of the intervertebral disc, sciatica, prolapse, pelvic inflammatory disease, or lumbar disc herniation [1]. Lumbar pain is a national issue accounting for approximately $50 billion in health care costs and the loss of 264 million work days across the American workforce [2]. 80% of the American population is expected to experience lower back pain at some point in their lives, and the global incidence of lower back pain has increased by over 50%. [2]. Mild back pain can be treated with painkillers such as Tylenol (acetaminophen) [3], but debilitating back pain - which renders the victim incapable of work or play - requires costly and dangerous surgical treatment. Advancements in medicine should aim to discover and optimize treatment options that are safer, more reliable, and more cost-efficient.

One of the leading causes of debilitating back pain is lumbar intervertebral disc herniation. Lumbar disc herniation is when a small portion of the intervertebral disc in between the vertebrae of the lower spine is squeezed or pinched out of its normal position and pushes up against a spinal nerve, stimulating it and causing pain. Risk factors for lumbar disc herniation include age, gender, and occupation. LDH is most common in men between the ages of 35-50 and workers in physically demanding jobs. Frequent heavy lifting causes repeated mechanical loading of the intervertebral disc, plastic deformation, and ultimately fatigue failure [2]. If the stress caused by the mechanical loading exceeds the yield stress, the disc will deform and bulge, thereby putting pressure on the spinal nerves. By pushing up against the spinal column, the herniated disc stimulates the pressured spinal neurons to fire, and creates a myriad of symptoms including a dull or sharp back pain, leg pain, and foot pain.

Treatment of LDH includes physical therapy, painkiller prescription, corticosteroid injection and surgical removal or discectomy. The first three treatments are conservative, and only useful for mild cases of lumbar pain. For debilitating lumbar pain, full surgical intervention is now viable, but undesirable due to having a long recovery time and post-operative complications. An intermediate, more practical solution to lumbar disc herniation called microdiscectomy, also known as laparoscopic discectomy or endoscopic discectomy, was adopted in the 1990s which mechanically removes the herniated region of the disc, thereby relieving pain on the spinal nerve [4]. However, a similar, novel procedure called laser discectomy has emerged as a minimally-invasive solution with faster recovery and higher success rates.

Laser discectomy uses Light Amplification by Stimulated Emission of Radiation (Laser) to focus infrared light on the herniated disc tissue to heat and vaporize the tissue [5][6]. By thermally reducing the mass of the intervertebral disc, also known as thermal ablation, the pressure on the spinal nerve is reduced and pain is alleviated. The energy density of the laser determines how efficiently and quickly it heats up and vaporizes the targeted tissue. The surgical precision of the laser, which surpasses that of microdiscectomy, allows it to be minimally invasive and reduce collateral damage as compared to other surgical methods. Additionally, procedure time of laser discectomy procedure is roughly 2 hours compared to the 4 hours of the more invasive procedures. In total, both the precision and quickness of laser discectomy make it an attractive alternative to more conventional herniated disc removal methods.

While lasers present an attractive alternative to conventional procedures, care must be taken when choosing the correct administration parameters for the laser. Each laser can emit pulses at a definite wavelength, amplitude, and separation. The wavelength used in LDH laser discectomy is usually 2.1 microns (from the Ho:YAG laser) [7]. The amplitude or power of the pulse must be chosen so that it is high enough to vaporize the correct amount of herniated tissue but low enough to minimize thermal damage to nearby healthy tissue. The separation time between pulses must also be chosen to not build up and transfer excess energy to surrounding tissue. Moreover, the laser parameters may need to vary between patients, as disc tissue density and degree of bulging is highly variable.

A balance must be struck between the time required for the application of the laser and the laser power, both of which determine the amount of ablated tissue and the extent of thermal damage to the adjacent vertebrae and intervertebral disc tissue. Since the composition of the vertebral disc is mostly water [8], the temperature that needs to be reached to ablate tissue is around 130°C, slightly higher than the temperature at which water evaporates. However, when the temperature of adjacent tissue increases beyond 46°C, irreversible cell damage begins to occur. Between 46°C and 52°C the risk for localized microvascular thrombosis, ischemia, and hypoxia increases. Once temperature reaches 60-65°C, denaturation and necrosis of tissues begins, resulting in tissue inflammation and scar tissue formation. [6] At this point, the functionality and mechanical properties of the tissue have most likely been irreversibly compromised.

Laser discectomy for treatment of lumbar disc herniated presents several improvements to more conventional methods. However, carefulness must be taken when choosing the correct laser parameters, as these can directly affect the amount of tissue that is vaporized. Done properly, laser discectomy can offer a low-risk, high-reward method to treat herniated discs.

2.1 Problem Statement

The purpose of this study is to investigate the suitable laser power and operating time to optimize the performance of laser spinal surgery in treating herniated discs. The transfer of energy from the laser to the herniated disc tissue almost instantaneously vaporizes the tissue. This removes the portion of the herniated disc impinging and pushing on the spinal nerve. With an adequate treatment time, enough disc tissue can be removed to alleviate pain while also ensuring that local vertebral tissue is not thermally damaged. Therefore, it is necessary to model the temperature

profile of a herniated disc and surrounding vertebrae to ensure successful laser ablation while minimizing adverse effects. Subsequently, it is important to measure the effects of varying model parameters such as thermal conductivity, laser power, and refractive index on the optimality and practicality of the laser surgery.

2.2 Design Objectives

The goals for this project are as follows:

- ➢ Model the temperature profile in a herniated disc-vertebral region by simulating laser ablation under physiological conditions.
- ➢ Determine the maximum amount of disc tissue that can be safely removed
- ➢ Perform a sensitivity analysis of various parameters in LDH laser ablation to identify any high-impact parameters
- ➢ Find the optimal procedure time that maximizes disc tissue removed while minimizing unnecessary thermal damage

3. Methods

3.1 Schematic

A 3-D slab geometry was implemented into COMSOL Multiphysics® to model a herniated disc in between two vertebrae. While a normal intervertebral disc has a cylindrical geometry, a real herniation deviates from the curved geometry and a real surgery would make a near-rectangular incision. Thus a Cartesian geometry was adopted. The computational domain is chosen to approximate an intervertebral disc with a herniated region and vertebral bone regions (see Fig.1).

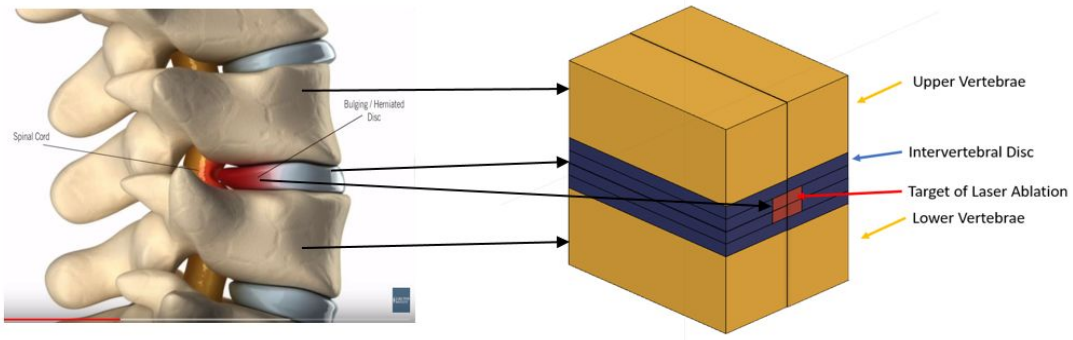

Figure 1: 3-dimensional schematic of the computational domain with two planes of symmetry. The yellow region represents healthy vertebral tissue. The blue region represents healthy intervertebral disc tissue that is not directly heated by the laser. The red region represents herniated intervertebral disc tissue that is target of laser ablation.

The model in Fig. 1 also has two planes of symmetry, allowing computation time to be reduced by a factor of four and resulting in Fig. 2. Dimensions were chosen based on anatomical parameters, and proximity to the laser ablation region. These proximate regions must contain all the thermal affliction and show no temperature change at its boundaries in order to minimize necrosis of healthy tissue. Post processing confirmed that this domain size was sufficient.

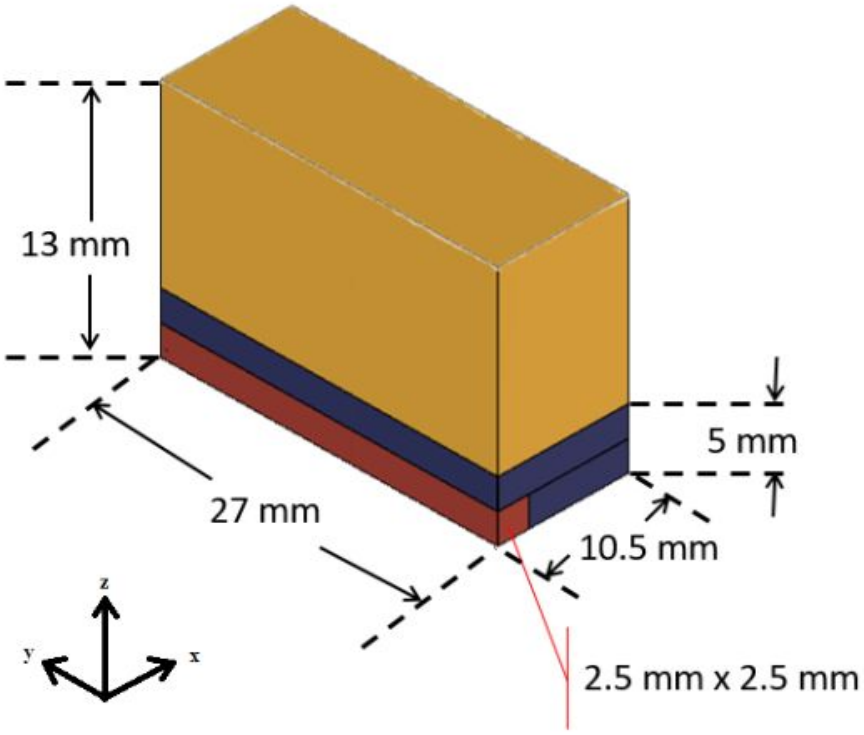

Figure 2: 3-dimensional schematic of the computational domain accounting for symmetry showing dimensions (mm). The yellow region represents healthy vertebral tissue. The blue region represents healthy intervertebral disc tissue that is not directly heated by the laser. The red region represents herniated intervertebral disc tissue that is the target of laser ablation.

Computational Domain:

$0 < x < 10.5$ mm

$0 < y < y_{surface} = 27$ mm at t = 0 (boundary deforms)

$0 < z < 13$ mm

3.2 Variables

The variables utilized in the governing equations and boundary conditions are listed along with their units and descriptions. (Table 1) The values used for the input parameters can be found in Table 2 of Appendix A.

Table 1: Variables used in governing equations

Symbol	Units	Description
T	K	Temperature
t	s	Time
ρ	$kg\ m^{-3}$	Density
C_p	$J\ kg^{-1}\ K^{-1}$	Specific Heat
k	$W\ m^{-1}\ K^{-1}$	Thermal Conductivity
$Q_{ablation}$	J	Volumetric Heat Generation by Laser
$Q_{evaporation}$	J	Volumetric Heat Loss by Vaporization
P	$W\ m^{-2}$	Laser Power
μ_s	m^{-1}	Scattering Coefficient
μ_a	m^{-1}	Absorption Coefficient
g	Unitless	Anisotropy Coefficient
r	Unitless	Ratio of Reflected Light to Laser Power
c_*	$m\ s^{-1}$	Speed of Light in Material
c_0	$m\ s^{-1}$	Speed of Light in Vacuum
N	Unitless	Refractive Index
n	m	Direction of Normal to Surface
λ	$J\ g^{-1}$	Enthalpy of Vaporization
D	$m^2\ s^{-1}$	Optical Diffusion Coefficient
ϕ	$W\ m^{-2}$	Fluence Rate
M	$kg\ s^{-1}$	Rate of Mass Loss
V_{lost}	m^{-3}	Volume Lost from Ablation
V	m^{-3}	Total Volume
R	unitless	Reflectance

3.3 Governing Equations

The laser ablation heating process can be modeled with the 3D transient heat transfer equation without convection (Eq. 1). Metabolic heat generation is considered negligible, and the entire region has no fluid flow. Since an infrared laser has significant penetration depth and scattering in tissue [10], its heating effect is implemented as volumetric heat generation coupled with an optical diffusion equation. Laser obstruction from tissue vapor is considered negligible. To mimic the destruction of tissue, a moving surface equation was implemented in which the mesh

conditionally deformed at ablation temperature and a volumetric loss equation was used to measure ablation rate.

The computational domain of the process also consists of three subdomains undergoing variations on this physics and is thus the governing equations in each domain uses varied parameters or boundary conditions. For example, the appropriate tissue parameters, k, ρ, and c_p is applied to vertebral and intervertebral disc tissue when computing heat transfer for each region.

Transient 3D Heat Transfer in Cartesian Coordinate System:

$$\rho c_p \frac{\partial T}{\partial t} = k\left(\frac{\partial^2 T}{\partial x^2} + \frac{\partial^2 T}{\partial y^2} + \frac{\partial^2 T}{\partial z^2}\right) + Q_{ablation} - Q_{evaporation} \qquad \text{(Eq. 1)}$$

$Q_{ablation}$ (Eq. 2) is dependent on the energy transferred from the laser to the tissue, which requires fluent rate to be known throughout the system. Thus this governing equation is coupled with another governing equation for the "diffusion" of the laser energy via:

$$Q_{ablation} = \mu_a \varphi \qquad \text{(Eq. 2)}$$

$Q_{evaporation}$ (Eq. 3) is the energy removed from the system due to the vaporization of tissue. Since this only occurs at regions where the temperature is high enough for ablation, it is described using the Heaviside step function (Eq. 4), where H(x) is 1 if x is positive and zero if x is negative:

$$Q_{evaporation} = M\lambda H(T - T_a) = \rho \frac{d}{dt}\left(\frac{V_{lost}}{V}\right)\lambda H(T - T_a) \qquad \text{(Eq. 3)}$$

$$\text{where, } H(T - T_a) = \begin{cases} 1 \text{ if } T - T_a \geq 0 \\ 0 \quad \text{otherwise} \end{cases} \qquad \text{(Eq. 4)}$$

See Volumetric Loss Governing Equation section for calculation of V_{lost}.

Light Optical Diffusion Governing Equation:

The light optical diffusion model (Eq. 5) can be used to describe light transport and calculate the heat generation source term in the intervertebral tissue. The fluence rate of the laser in the intervertebral disc is mostly determined by absorption and scattering, although anisotropy and refractive index are also a factor.

$$\frac{\partial \varphi}{\partial t} - D\nabla^2 \phi + c_* \mu_a \varphi = 0 \qquad \text{(Eq. 5)}$$

$$\text{where, } D = c_* [3 (\mu_a + (1-g) \mu_s)]^{-1}$$
$$\text{and } c_* = c_0 N^{-1}$$

Volumetric Loss Governing Equation:

To measure volumetric loss for validation, the entire domain is integrated for regions where the temperature (T) of the tissue exceeds the ablation temperature (T_a) accumulating over time as shown in Equation 6. This also utilized the Heaviside function (Eq. 4).

$$V_{lost} = \iiint H(T - T_a)\, dV \qquad \text{(Eq. 6)}$$

To convert the volume of tissue ablated to mass of tissue ablated, the volumetric loss was multiplied by the density of the tissue (Eq. 7).

$$M = \rho \frac{d}{dt}(V_{lost}) \qquad \text{(Eq. 7)}$$

Deforming Geometry Governing Equation:

The physical process of the deforming geometry is modeled mathematically as a velocity equation (Eq. 8). Assuming that the surface velocity is only in the y-direction, the velocity at which the surface deforms is dependent on the fluence of the laser as well as the density and isobaric specific heat of the tissue. This equation is only applied at nodes which are at temperatures exceeding the ablation temperature.

$$\frac{\partial y}{\partial t} = \frac{\Phi}{\rho c_p} \qquad \text{(Eq. 8)}$$

3.4 Boundary Conditions

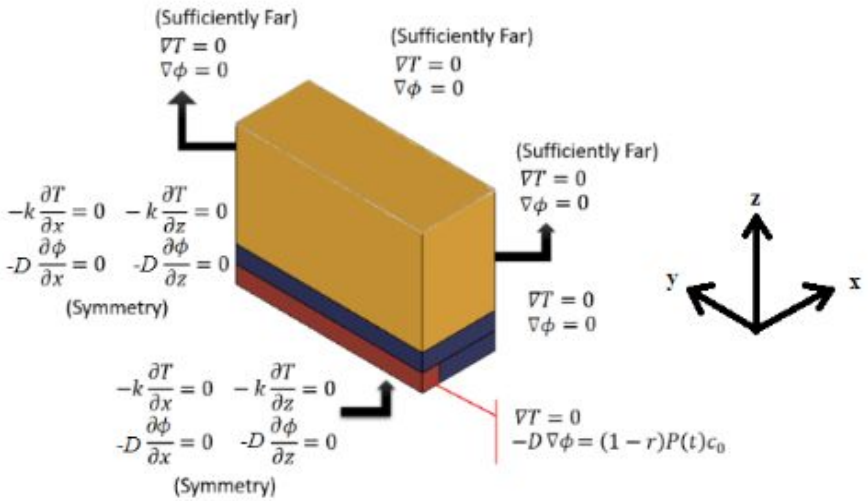

Figure 3: Schematic of computational domain annotated with boundary conditions. The yellow region represents healthy vertebral tissue. The blue region represents healthy intervertebral disc tissue that is not directly heated by the laser. The red region represents herniated intervertebral disc tissue that is susceptible to direct ablation heated by the laser.

For heat transfer:
The boundary conditions implemented are a zero temperature gradient condition far way and a zero heat flux condition at the two planes of symmetry.

$T(x \to \infty) = 310$ K (x is far enough that no thermal variation occurs)
$T(y \to \infty) = 310$ K (y is far enough that no thermal variation occurs)
$T(z \to \infty) = 310$ K (z is far enough that no thermal variation occurs)
$-k\frac{\partial T}{\partial x}|_{x=0} = 0$ (due to symmetry)
$-k\frac{\partial T}{\partial z}|_{z=0} = 0$ (due to symmetry)

For optical diffusion:
Equation 11 represents the boundary condition on the intervertebral disc tissue surface receiving laser radiation, where P(t) is laser irradiance as a function of time. This model uses a constant and non-pulsating laser power so, P(t) = P. The subsequent boundary conditions include a zero (light) concentration gradient condition far away, and a zero laser flux boundary condition at the two planes of symmetry.

$(1-r)\, P(t)\, c_0 = -D\frac{d\phi}{dn}$ (Eq. 11)
$\phi(x \to \infty) = 0$ (x is far enough that no fluence variation occurs)
$\phi(y \to \infty) = 0$ (y is far enough that no fluence variation occurs)
$\phi(z \to \infty) = 0$ (z is far enough that no fluence variation occurs)
$-D\frac{\partial \phi}{\partial x}|_{x=0} = 0$ (due to symmetry)
$-D\frac{\partial \phi}{\partial z}|_{z=0} = 0$ (due to symmetry)

When the temperature at a node reaches the ablation temperature, that node is then removed from the computational domain, permanently changing the mesh. The boundary condition must be adjusted such that the optical diffusion boundary condition due to the application of the laser must be applied to the new surface, which becomes irregular since the ablation process does not occur evenly across the surface of the domain.

3.5 Initial Conditions

At the beginning of the simulation, the entire computational domain is assumed to be at standard body temperature (310 K) and devoid of any laser fluence.

$T|_{x,y,z}(t = 0) = 310$ K
$\phi|_{x,y,z}(t = 0) = 0$ W · m^{-2}

4. Results & Discussion

4.1 Mesh Convergence Analysis

For the computational model that has a moving boundary with deforming geometry, a uniformly extra coarse mesh was constructed using free triangular elements (Fig. 4). The internal region is also filled and meshed, as shown in Fig 5. A finer mesh was not chosen as the baseline computation model solely to conserve computational time.

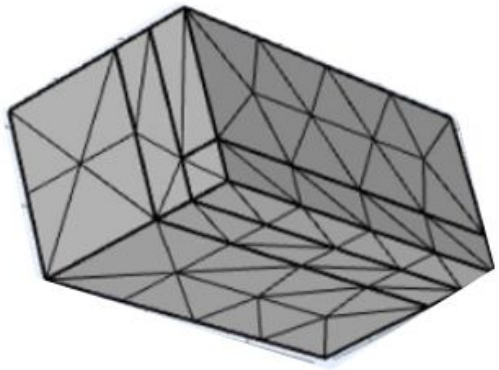

Figure 4: Uniformly extremely coarse mesh. Mesh consists of 20 vertex elements, 46 edge elements, 70 boundary elements, and a total of 62 elements. The minimum element quality was 0.1058.

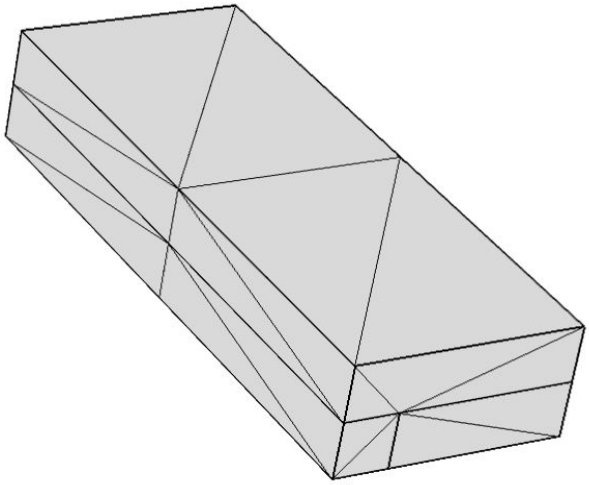

Figure 5: Uniformly extremely coarse mesh with top vertebrae block removed. Mesh reveals the subsurface or internal mesh with free triangular elements of the partial computational domain.

The simulation was subsequently performed using an extremely coarse, extra coarse, coarser, and coarse mesh. A mesh convergence analysis was performed by determining the number of mesh elements required for the average mass of tissue ablated to remain constant. Fig 6 shows that mesh convergence occurs at approximately 800 mesh elements.

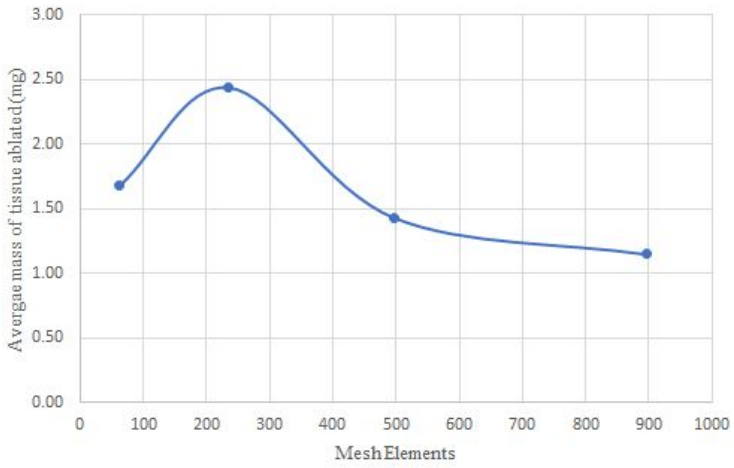

Figure 6: Mesh convergence analysis plot. Surface average mass of tissue ablated is plotted against the number of mesh elements.

4.2 Temperature Profiles

As the laser is applied temperature increases especially in the herniated intervertebral disc region. After 5 seconds , the maximum surface average temperature rises to 402K, which is above the ablation temperature of the intervertebral disc. Hence, ablation begins at some point after 5 seconds and can be seen by the deforming geometry and moving mesh at the 10 second mark.

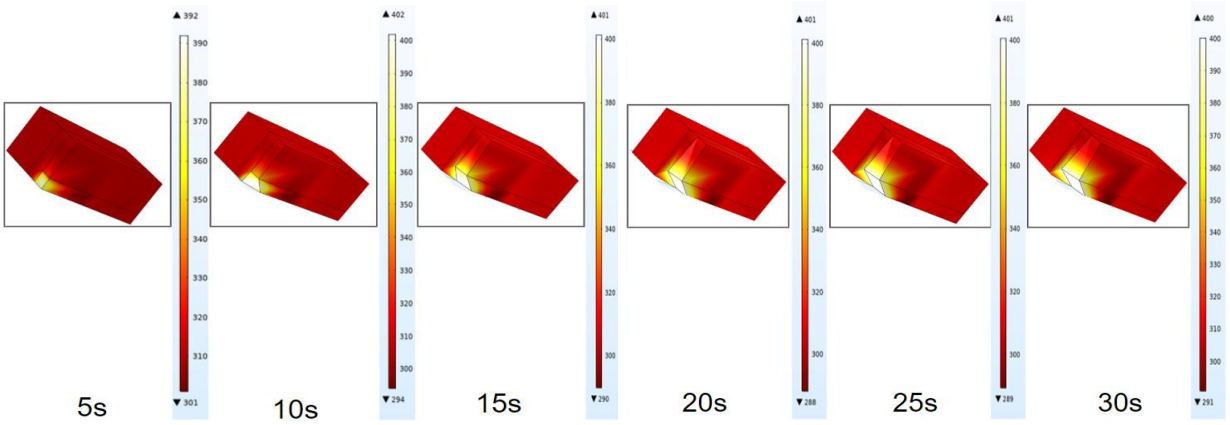

Figure 7: Surface temperature plots at various times showing changes in temperature as the laser is continuously applied. The deforming geometry or moving boundary can also be seen as the simulation progresses. Different Kelvin temperature scales are provided at each time point since the temperature profiles change over time.

4.3 Tissue Ablation

The physical process of mass loss due to tissue ablation only occurs when the temperature of the tissue exceeds the temperature of ablation. Since the entire computational domain is assumed to initially be at normal body temperature (310 K), the energy absorbed by the tissue due to the application of the laser is used to raise the temperature of the tissue to the ablation temperature, which is assumed to be 400K. Once the temperature of the tissue reaches the ablation temperature, energy must then be used for the phase transition of the solid tissue to vaporized tissue, which is dependent on the enthalpy of vaporization. Therefore, the mass loss does not begin until approximately 6.2 seconds. (Fig. 8). Between approximately 6.2 seconds and 7.2 seconds, the mass loss occurs at a constant rate. However, after 7.2 seconds, a higher rate of mass loss occurs, indicated by the increase in steepness of the graph. After approximately 7.2 seconds, a greater proportion of the total computational domain has reached temperatures approaching the ablation temperature due to conductive heat transfer, allowing for tissue to be ablated at a higher rate.

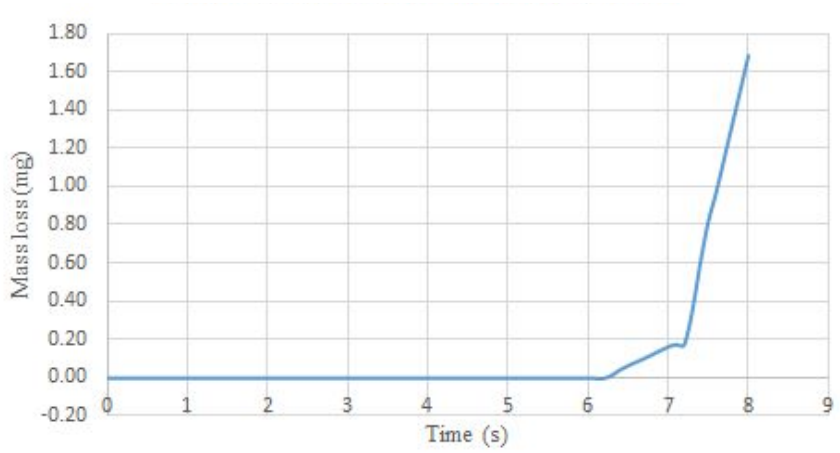

Figure 8: Plot of total tissue ablation over time. Plot of mass of intervertebral tissue ablated or lost over 8 seconds, showing the time at which tissue ablation begins and the total amount of tissue ablated at any given time.

4.4 Validation

Validation of the model was carried out by comparing the computational data for the ablation rate or mass loss data for the intervertebral disc with data from Buchelt et al. [9]. The quantitative results of disc ablation were graphed as mass loss (mg) versus total energy applied (joules). The plots generated in this study reveal that the directly proportional relationship between mass loss and total energy applied is accurately modeled. (Fig. 9) However, discrepancies in the mass loss profiles can be attributed to biological variation and non-uniformity in heat transfer properties, variability in the tissue ablation point in reality, and

differences in the laser parameters, which can be explored more in depth through sensitivity analyses.

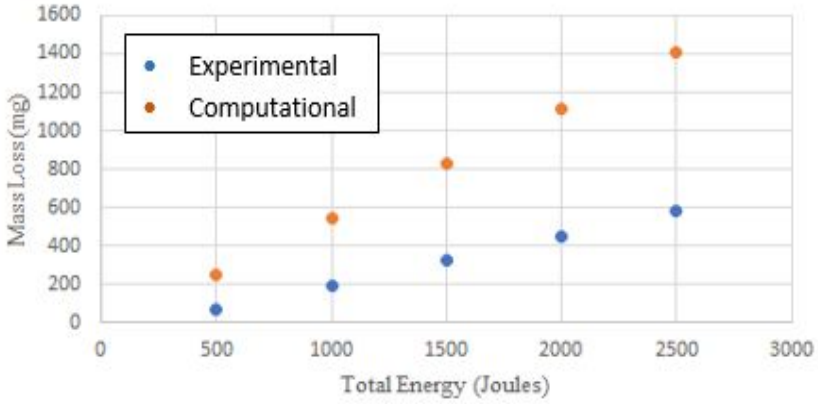

Figure 9: Validation of the model using experimental and computational data of ablation rates (mass loss) using a 10W laser. Joules (x-axis) is the total energy transferred from the process, which corresponds to time.

The model seems to be valid for early times where a relatively small amount of total energy was absorbed by the tissue since the discrepancy in the mass loss between the experimental and computational data is minimal. However, as time increases and the amount of energy absorbed by the tissue increases, the discrepancy between the experimental and computational data increases. There are multiple reasons that could explain the increasing discrepancy in the data. The main reason for the discrepancy was the extrapolation of mass loss data for long times which translates to when a large amount of energy has been absorbed by the tissue. Another reason for the discrepancy could have been the use of a 3-dimensional Cartesian geometry, which simplifies the actual cylindrical geometry intervertebral disc. Furthermore, biological variability in the material properties of the tissue could also contribute to the difference in mass loss as shown in the sensitivity analysis. These reasons may introduce physical approximation errors that are propagated for larger times.

4.5 Sensitivity Analysis

To perform sensitivity analysis is to vary a few parameters and see how these changes affect the dependent variable, the percentage of tissue ablated. More specifically, the density, thermal conductivity, and specific heat capacity of the intervertebral disc, as well as the laser power density were varied by +/-10 percent. Biological variability in the material properties of the intervertebral disc, due to age, gender, physical activity levels as well as other factors, are assumed to not exceed 10%. To optimize the laser discectomy procedure, variations in either the laser heat generation term and laser pulse length would cause large deviations in our final model. This is because the heat generation of the laser is directly proportional to the velocity of the moving boundary. As the moving boundary is directly proportional to the laser heat terms, small changes in the laser parameter would greatly affect the rate of ablation. Through a thorough sensitivity analysis of these selected parameters, it is possible to determine the robustness of the

computational model . The specific parameters that the model is most sensitive to must be very accurately measured to ensure that there is an understanding of the flexibility allowed in carrying out the laser ablation procedure.

Sensitivity analysis of the computational model to the 4 parameters: density, thermal conductivity, specific heat capacity and laser power density. (Fig. 10)

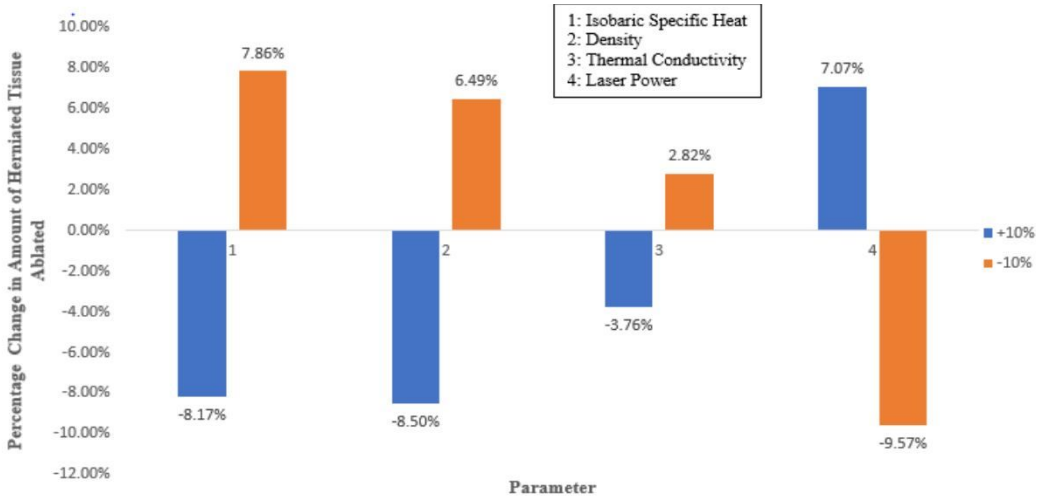

Figure 10: Sensitivity analysis performed by varying parameters by +/- 10 percent to analyze the effect on percentage of tissue ablated. Parameters tested include isobaric specific heat of intervertebral disc tissue (c_p), density of intervertebral disc tissue (ϱ), thermal conductivity of intervertebral disc tissue (k), and laser power density (P).

Each parameter was varied by increasing or decreasing their original value by 10% and then calculating the resulting percentage change in the amount of herniated tissue ablated. As shown in Fig. 10, increasing isobaric specific heat, density, and thermal conductivity of the intervertebral disc all resulted in a decrease in the percentage of herniated tissue ablated. This lines up with projected expectations as an increase in specific heat suggests that a greater amount of energy is required to bring the temperature of the tissue to the ablation temperature. This in turn increases the amount of energy required for the ablation of tissue and a subsequent decrease in the total amount of tissue ablated.

Increasing the density of the intervertebral tissue results in the ablation region of interest having a more concentrated composition of its constituents. These constituents are more densely packed and exhibit stronger intermolecular forces that increase their stability and resistance to bond cleavage via increasing molecular kinetic energy. Thus, higher density of the intervertebral disc translates to a larger amount of energy required to disrupt bond stability and evaporate tissue.

Increasing the thermal conductivity of the intervertebral tissue reduced the amount of tissue ablated because the physical transfer of heat throughout the tissue via molecular collisions increased. As a result, the temperature of the tissue increased less quickly, more energy was required for the tissue to reach the temperature of ablation, and less tissue was ablated.

Increasing laser power density increases the amount of energy that is applied to the system from the laser. An increase of energy applied to the system leads to more heat transfer to the herniated tissue and therefore a larger percentage of the tissue will reach the specified ablation temperature. Thus, as Fig. 10 shows, increasing laser power density will increase the amount of herniated tissue that is ablated.

As shown in Fig. 10, increasing isobaric specific heat, density, and thermal conductivity of the intervertebral disc all resulted in a decrease in the percentage of herniated tissue ablated. On the other hand, increasing laser power density resulted in an increase in the percentage of herniated tissue ablated. These findings line up with what was expected for the aforementioned reasons. The largest variation in the result was observed by decreasing laser power density by 10% which caused a -9.57% decrease in the percentage change in the amount of herniated tissue ablated. As expected, the results of the simulation are most sensitive to laser power density parameters which can then be relatively easily manipulated to optimize the ablation procedure.

4.6 Optimization

To determine the optimal time for the laser ablation procedure, a cost function, J, was defined as the difference between the two functions, F(t) and G(t). F(t) represents the total percentage of intervertebral disc tissue damaged as a function of time, while G(t) represents the total percentage of intervertebral disc and vertebral tissue damaged as a function of time. Tissue is considered "damaged" if its temperature exceeds the necrosis temperature of 350K. Therefore, to optimize the procedure, the difference between F(t) and G(t) should be maximized as represented by Equation 12.

$$J = \max (F(t) - G(t)) \qquad \text{(Eq. 12)}$$

Time optimization of the laser discectomy occurs at approximately equal to 10.9s, assuming constant laser parameters and material properties (Fig. 11). At times other than 10.9s, the difference in the amount of damaged herniated intervertebral tissue and the amount of healthy tissue damaged is not optimal. At shorter times, the amount of herniated intervertebral disc tissue damaged may not have reached the optimal amount since energy is both required for the increase in temperature of the tissue as well as the phase transition of the tissue. At longer times, the amount of damaged herniated intervertebral disc tissue continues to increase. However, heat dissipation from the disc region and conduction increases the amount of surrounding vertebral tissue that reach the temperature at which thermal damage begins to occur. Thus, the value of the optimization function decreases after 10.9 seconds.

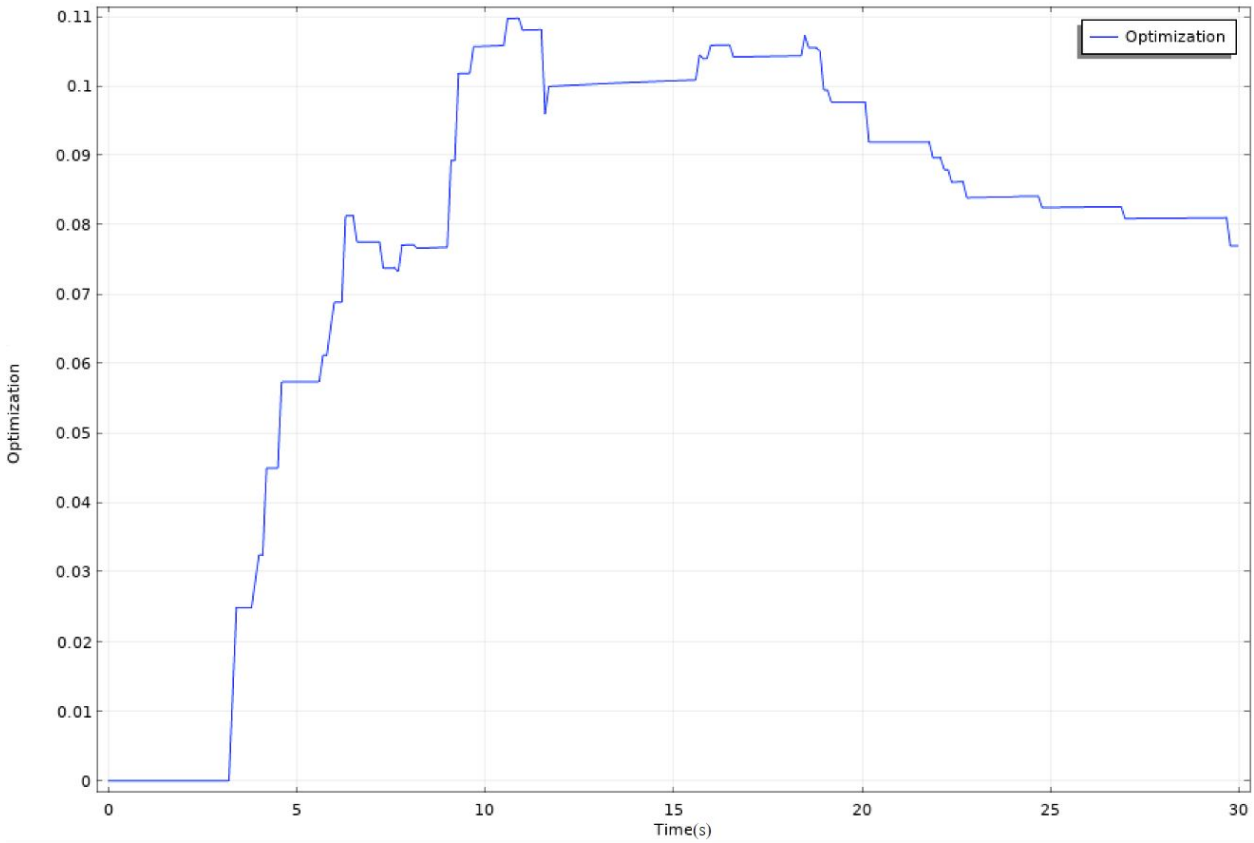

Figure 11. Plot of the optimization cost function, J, to determine the optimal amount of time for the laser ablation procedure, assuming constant laser parameters and material properties. The cost function is maximized when time is approximately equal to 10.9 seconds.

5. Conclusions & Design Recommendations

5.1 Implications

In this model, 3D heat transfer of laser lumbar discectomy using a Ho:YAG laser (2.1 micrometer wavelength at 9 Watts) was studied. In modeling the heat transfer and optical diffusion from the laser energy source, a quantifiable approximation was made for the optimal time to carry out this procedure. A sensitivity analysis was also performed and revealed that the density and the laser power were the two parameters that the mass loss was most affected by. This suggests that highly accurate data for the density of the intervertebral tissue and the laser power are crucial for replicating and implementing the results of this study. Furthermore, the safeness and optimization of the procedure are also dependent on the precision and accuracy of these parameters since small changes in these parameters could result in unsafe or non-optimal tissue losses.

Validation of the model could only be achieved for small amounts of total energy absorbed by the tissue. The current model, with the given logistical constraints, could only be run for a few hours a day resulting in an 8 second simulation and a total joule transfer of 72 joules. The

literature reported the lowest exact joule-transfer to mass-loss values at 400 to 500 joules. As the extrapolation increased the percent error also increased systematically indicating a propagation of some cause of error. The most likely cause for this is the use of constant material property values instead of temperature-dependent values as they are in living systems. This would feasibly result in an increasing systematic error. Computational error should be negligible and discretization error is minimized by the mesh convergence. Physical approximation error is also a possible cause, but this would more likely lead to constant (or decreasing as the ablation progresses inwards) systematic error. Longer simulations without the need for extrapolation are necessary for a proper validation and more insight into the issue,. A significant implementation for future models would be the usage of temperature dependent material properties for the disc and vertebral tissue.

Sensitivity analysis revealed that the two most significant parameters were laser power density and intervertebral disc density respectively. Pressure-constant specific heat was also a close-third in significance on result impact. Laser power density is an easily controllable independent variable for laser discectomy. Future models can attempts to simulate laser ablation at different laser powers and see if the same effect can be achieved at a lower cost. However, the high sensitivity to laser power density in the surgery means that the device emitting the laser must be extremely precise, and it is worth investing extra money and care into making sure that the device operates as necessary. The sensitivities to density and specific heat are also of importance because they are not easily controlled nor predictable variables. There may be significant individual variation within patients, even without clinical manifestation. If this treatment is to be provided to a wider community then a more personalized approach must be taken. Personalized medicine is a contemporary treatment ideology where a patient's exact genetic and chemical compositions should be measured before treatment and taken into account. Until now, only a few essential factors were measured. This sensitivity analysis supports that individual variation in disc and vertebrae are critical in performing laser lumbar discectomy, and that personalized medicine may be necessary for safe and adequate treatment.

Optimization of the laser ablation versus time showed that the most efficient ablation occurred at 10.9 seconds into the simulation. It is crucial for the optimal time to be factored into the surgical procedure to ensure that an adequate amount of herniated intervertebral disc tissue is removed, while the amount of surrounding healthy vertebral tissue damaged is minimized. Given the biological variability in tissue material properties, the optimal time for the ablation procedure may vary person . Variability in the size of the herniated discs may necessitate a greater amount of tissue removal, which means that the ablation time needs to be optimized on a case-by-case basis.

5.2 Limitations, Recommendations and Future Improvements

The computational model aims to minimize the potential harm that can be caused by laser lumbar discectomy by finding optimal laser parameters. By determining these optimal conditions for the laser discectomy, this can reduce the average cost of the procedure by minimizing the risks of the procedure, reducing the risk of future complications. Since the amount of tissue removed is sufficient to relieve pressure on the surrounding nerves. As a result, patients who are

treated with lumbar discectomy can perform their daily activities without experiencing constant lumbar pain. The cost of the procedure also depends on the operating costs associated with using a laser and costs associated with the surgery, including anesthesia, staffing, etc.

In terms of the efficacy of the design of the laser discectomy procedure, a constant laser power was implemented. This model also provides computational data that could be used to determine the amount of laser ablation time to remove a desired amount of intervertebral disc tissue. A sensitivity analysis that considers biological variability of the material properties of the intervertebral disc tissue allows for some degree of uncertainty in the necessary time for the ablation procedure. In this report, optimization of the procedure to minimize thermal damage to surrounding tissue is also considered. This data can be used to maximize the efficacy and safety of the procedure. It should be noted that the procedure may not be suitable for patients with degenerative disc disease as drastic changes in material properties and wear accumulation of the intervertebral disc may increase the risk of future complications.

User friendliness of the laser ablation procedure depends on the expertise of the neurosurgeon and the accuracy and precision of the laser instrument. In general, laser instruments used in a medical setting are highly precise and are constantly being improved for use in minimally invasive procedures. The physics of lasers and laser properties, such as the effective optical penetration depth of the laser in biological tissues, are well-studied and understood. Thus, the application of the results of this study could be easily implemented in current practices in the treatment of intervertebral discs.

The computational model presented in this paper is based on the use of a single type of laser (Ho:YAG) at a given laser power, which limits the scope of this research. To address this concern, there are many future improvements and alterations to this existing model to allow for further analysis and optimization. Since only COMSOL Multiphysics was used in this simulation, other computational modeling software, such as ADINA, Fluent inc., and Nastran, may be used for additional evidence to support the accuracy of the model. These multiphysics modeling programs may be used to generate temperature profiles that would help confirm that the heat transfer physics is accurately modeled in COMSOL.

An analysis of other types of lasers for application to laser discectomy may reveal other avenues for further optimization and validation of the COMSOL model by broadening the literature available for comparison. The COMSOL model could also be further optimized by directly implementing a pulsating laser to increase the safeness of the procedure by implementing better control over temperature.

Mesh refinement using a user-defined mesh that is tailored to the laser ablation process. A greater density of mesh should be present closer to the surface where the laser is directly applied. However, mesh refinement could significantly increase computation time, which is dependent on the mesh size and distribution. Modeling the heat transfer and ablation processes using more accurate 3D geometry could be performed by using imported CT scans from medical image databases such as lifescience.db and refining with softwares such as MeshLab for mesh processing and SolidWorks for creation of a 3D solid that can be imported into COMSOL

Multiphysics. Implementing more complex geometries into a computational model could also significantly increase computation time. Inclusion of metabolic heat generation and slight convection heat transfer due to the ablation process could also improve the accuracy of the modeling of the heat transfer process. A probabilistic modeling of the ablation process could be implemented since not all tissue ablates at exactly 400K. Analysis of this alteration could reveal whether the total amount of tissue ablated changes significantly.

Appendix A: Input Parameters

Table 2: A list of input parameters used in the model

Parameter	Symbol	Value	Units	Source
Intervertebral Disc Properties				
Dimensions	(x,y,z)	(10.5, 27.0, 5.0)	(mm, mm, mm)	[11]
Thermal conductivity	k	0.21	$W\ m^{-1}\ K^{-1}$	[12]
Density	ϱ	1100	$kg\ m^{-3}$	[13]
Isobaric specific heat	C_P	3200	$J\ kg^{-1}\ K^{-1}$	[13]
Enthalpy of vaporization	λ	1489.75	$J\ g^{-1}$	[14][16]
Index of refraction	N	1.39	Unitless	[15]
Ablation Temperature	T_a	400	K	[16]
Vertebrae Properties				
Dimensions	(x,y,z)	(10.5, 27.0, 8.0)	(mm, mm, mm)	[17]
Thermal conductivity	k	0.55	$W\ m^{-1}\ K^{-1}$	[18]
Density	ϱ	1900	$kg\ m^{-3}$	[19]
Isobaric specific heat	C_P	1256.04	$J\ kg^{-1}\ K^{-1}$	[18]
Laser Properties				
Scattering coefficient	μ_s	60	cm^{-1}	[15]
Absorption coefficient	μ_a	9.65	cm^{-1}	[15]
Optical Anisotropy factor	g	1	Unitless	[15]
Laser Penetration Depth	δy_{laser}	0.5	cm	[20]
Laser Power Density	P	1080	$W\ m^{-2}$	Calculated
Reflectance	R	0.026627685	Unitless	Calculated
Optical Diffusion Coefficient	D	$7.447 \cdot 10^4$	$m^2 s^{-1}$	Calculated
Speed of light in vacuum	c_0	$2.997 \cdot 10^8$	$m\ s^{-1}$	[21]
Speed of light in tissue	c_*	$2.156 \cdot 10^8$	$m\ s^{-1}$	Calculated
Ratio of reflected light to laser power output	r	$2.466 \cdot 10^{-5}$	Unitless	Calculated

Appendix B: Computation Specifications

COMSOL Multiphysics® 5.4 was executed on a Macbook Pro with 16 GB RAM and Intel i7 processor, and implemented the finite element method with MUMPS equation system solver. An average simulation took 3 hours and 1.81 GB RAM to complete. The following simulation was run shorter to demonstrate the computational specifications.

```
Time-stepping completed.
Solution time: 855 s. (14 minutes, 15 seconds)
Physical memory: 1.18 GB
Virtual memory: 7.11 GB
Ended at May 7, 2019 6:54:19 PM.
----- Time-Dependent Solver 1 in Study 1/Solution 1 (sol1)
```

Appendix C: Mathematical Equations and Calculations

Laser power density: $P = \frac{Q_0 T_p H}{A*(1s)} = \frac{(9J)(300\mu s)(10Hz)}{(25mm^2)(1s)} = 1080\ Wm^{-2}$

Reflectance: $R = (\frac{n-1}{n+1})^2 \approx 0.026627685$

Reflective ratio: $r = \frac{R}{P_0} = \frac{(\frac{n-1}{n+1})^2}{P} \approx \frac{0.026627685}{1080} = 0.000024655$

Optical Diffusion coefficient: $D = c_* [\ 3(\ \mu_a + (1-g)\ \mu_s)\ ]^{-1} =$

$= (\ 2.156 \cdot 10^8\ \text{m s}^{-1})[\ 3(\ 9.65\ \text{cm}^{-1} + (1\text{-}1)\ 60\ \text{cm}^{-1})\ ]^{-1} = \ 7.447 \cdot 10^4\ \text{m}^2\text{s}^{-1}$

Speed of light in tissue: $c_* = c_0 N^{-1} = (2.997 \cdot 10^8\ \text{m s}^{-1})\ (1.39^{-1}) = 2.156 \cdot 10^8\ \text{m s}^{-1}$

General heat transfer equation: $\rho c_p \frac{\partial T}{\partial t} + \nabla \bullet (uT) = \nabla \bullet (k \nabla T) + Q$

Model's heat transfer equation: $\rho c_p \frac{\partial T}{\partial t} = k(\frac{\partial^2 T}{\partial x^2} + \frac{\partial^2 T}{\partial y^2} + \frac{\partial^2 T}{\partial z^2}\ ) + Q_{ablation} - Q_{evaporation}$

Coupled heat source term: $Q_{ablation} = \ \mu_a \phi$

Coupled heat source term: $Q_{evaporation} = \ M \lambda H(T - T_a) = \ \rho \frac{d}{dt}(\frac{V_{lost}}{V}) \lambda H(T - T_a)$

Optical diffusion governing equation: $\frac{\partial \phi}{\partial t} - D \nabla^2 \phi + c_* \mu_a \phi = 0$

Volumetric loss governing equation: $V_{lost} = \ \iiint H(T - T_a)\ dV$

Mass loss equation: $M = \ \rho \frac{d}{dt}(V_{lost})$

Moving surface/deforming mesh governing equation: $\frac{dy}{dt} = \frac{1}{A} \frac{d}{dt}(V_{lost})$

Optimization function: $J = max(\ F(t)\ -\ G(t)\ )$

Appendix D: References

[1] Bethesda, MD. (Aug 7th, 2018). Low Back Pain Fact Sheet. *National Institute of Neurological Disorders and Stroke*. Retrieved March 15, 2019, from https://www.ninds.nih.gov/Disorders/Patient-Caregiver-Education/Fact-Sheets/Low-Back-Pain-Fact-Sheet

[2] American Chiropractic Association. (2019). Back Pain Facts and Statistics. Retrieved March 15, 2019, from https://www.acatoday.org/Patients/Health-Wellness-Information/Back-Pain-Facts-and-Statistics

[3] Ashner, Anne, CPT (Sep 24th, 2018). Taking Acetaminophen or Tylenol for Back Pain. Retrieved March 15, 2019, from https://www.verywellhealth.com/tylenol-and-acetaminophen-for-back-pain-297180

[4] Snyder, Laura, A., O'Toole, John, Eichholz, Kurt M., Perez-Cruet, Mick J., and Fessler, Richard (2014). The Technological Development of Minimally Invasive Spine Surgery. *BioMed Research International, vol. 2014, Article ID 293582, 9 pages*. 2014. Access at: https://doi.org/10.1155/2014/293582 Retrieved March 15th, 2019, from https://www.hindawi.com/journals/bmri/2014/293582/#sec3.2

[5] Gould, R. Gordon (1959). The LASER, Light Amplification by Stimulated Emission of Radiation". In Franken, P.A.; Sands R.H. (Eds.). *The Ann Arbor Conference on Optical Pumping, the University of Michigan, 15 June through 18 June 1959*. p. 128

[6] Datta, A.K. and V. Rakesh (2010). *An Introduction to Modeling of Transport Processes: Applications to Biomedical Systems*. Cambridge University Press. Retrieved March 15th, 2019.

[7] Jasvinder Chawla, MD, MBA (Aug 30, 2017). *Medscape*. Retrieved March 15, 2019, from https://emedicine.medscape.com/article/1145539-overview

[8] [5] Kenhub (2019). Intervertebral Discs. Retrieved March 15, 2019, from https://www.kenhub.com/en/library/anatomy/the-intervertebral-discs

[9] Buchelt, M., MD, Schlandmannm B., Schmolke, S., and Siebert, W., MD (1995). High Power Ho:YAG Laser Ablation of Intervertebral Discs: Effects on Ablation Rates and Temperature Profile. *Lasers in Surgery and Medicine 16,179-183*.

[10] Michael Ith, Martin Frenz, and Heinz P. Weber, (2001) "Scattering and thermal lensing of 2.12-µm laser radiation in biological tissue," Appl. Opt. **40**, 2216-2223

[11] Prithvi, R. (2008). Intervertebral Disc: Anatomy-Physiology-Pathophysiology-Treatment. Pain Practice, 8(1), 18-44. Retrieved May 5, 2019.

[12] Moghadam, M. N., Abdel-Sayed, P., Camine, V. M., & Pioletti, D. P. (2015). Impact of synovial fluid flow on temperature regulation in knee cartilage. Journal of Biomechanics, 48(2), 370-374. doi:10.1016/j.jbiomech.2014.11.008

[13] Park, J. S., Jung, Y. W., Choi, H., & Lee, A. (2018). VK-phantom male with 583 structures and female with 459 structures, based on the sectioned images of a male and a female, for computational dosimetry. Journal of Radiation Research, 59(3), 338-380. doi:10.1093/jrr/rry024

[14] Ignatieva, Natalia Yu. Zakharkina, Olga L. Andreeva, Irina V. Sobol, Emil N. Kamensky, Vladislav A. Myakov, Alexey V. Averkiev, Sergey V. Lunin, Valery V. (May 9th, 2007). IR Laser and Heat-induced Changed in Annulus Fibrosus Collagen Structure. Access at: https://doi.org/10.1111/j.1751-1097.2007.072.x

[15] Ignatieva, N. Y., Zakharkina, O. L., Andreeva, I. V., Sobol, E. N., Kamensky, V. A., Myakov, A. V., Averkiev, S. V. and Lunin, V. V. (2007), IR Laser and Heat‐induced Changes in Annulus Fibrosus Collagen Structure. Photochemistry and Photobiology, 83: 675-685. doi:10.1111/j.1751-1097.2007.072.x

[16] Iatridis, J. C., MacLean, J. J., O'Brien, M., & Stokes, I. A. (2007). Measurements of proteoglycan and water content distribution in human lumbar intervertebral discs. *Spine*, *32*(14), 1493–1497. doi:10.1097/BRS.0b013e318067dd3f

[17] Frobin, W., Brinckmann, P., Biggemann, M., Tillotson, M., & Burton, K. (1997). Precision measurement of disc height, vertebral height and sagittal plane displacement from lateral radiographic views of the lumbar spine. Clinical Biomechanics, 12. doi:10.1016/s0268-0033(96)00067-8 Copy Edit D

[18] S. Karmani. (2006). The thermal properties of bone and the effects of surgical intervention Curr. Orthop., 20 (1), pp. 52-58, 10.1016/j.cuor.2005.09.011

[19] Domán, I., & Illés, T. (2004). Thermal analysis of the human intervertebral disc. *Journal of Biochemical and Biophysical Methods, 61*(1-2), 207-214. doi:10.1016/j.jbbm.2004.06.004

[20] Ash, C., Dubec, M., Donne, K., & Bashford, T. (2017). Effect of wavelength and beam width on penetration in light-tissue interaction using computational methods. Lasers in Medical Science, 32(8), 1909-1918. doi:10.1007/s10103-017-2317-4

[21] Speed of light. (2019, April 12). Retrieved May 5, 2019, from https://en.wikipedia.org/wiki/Speed_of_light